Journal of Nuclear Materials 386–388 (2009) 56–59

Contents lists available at ScienceDirect

Journal of Nuclear Materials

journal homepage: www.elsevier.com/locate/jnucmat

# Atomistic modeling of nanosized Cr precipitate contribution to hardening in an Fe–Cr alloy

Jae-Hyeok Shim [a,*], Dong-Ik Kim [a], Woo-Sang Jung [a], Young Whan Cho [a], Brian D. Wirth [b]

[a] Materials Science and Technology Research Division, Korea Institute of Science and Technology, Seoul 136-791, Republic of Korea
[b] Department of Nuclear Engineering, University of California, Berkeley, CA 94720, USA

A B S T R A C T

Molecular dynamics simulations of the interaction between an edge dislocation and nanosized Cr precipitates in bcc Fe have been performed to investigate the hardening effect of α′ phases in high Cr ferritic/martensitic steels. The critical resolved shear stress needed for an edge dislocation to overcome Cr precipitates of diameter between 3 and 6 nm is larger than for dislocation glide in the bcc Fe lattice containing 10% Cr solute atoms. This indicates that the precipitation of α′ phases leads to hardening in high Cr ferritic/martensitic steels. The MD simulations reveal that the interspacing of Cr precipitates plays a more crucial role in the hardening of Fe–Cr alloys than the precipitate size. An attractive interaction exists between an edge dislocation and nanosized Cr precipitates, which is evident as a decrease in total energy when an edge dislocation is placed within in a Cr precipitate.



## 1. Introduction

7–12 wt.% Cr ferritic/martensitic steels are being considered as a structural material for future fusion and high temperature fission nuclear reactors due to their good mechanical properties at high temperatures and resistance to swelling [1]. It is well known that these steels suffer from irradiation hardening and embrittlement below irradiation temperatures of about 673 K, even at moderate dose. In order to ensure the long-term stability of these steels, it is important to understand their microstructural evolution and mechanical properties changes under high temperature and irradiation environment.

During neutron irradiation, it is known that fine (2–30 nm in diameter) bcc Cr-rich precipitates (α′) are formed in high Cr steels, in addition to clusters of vacancies and self-interstitial defects [2–7]. Little and Stow [2] used transmission electron microscopy (TEM) to characterize the critical Cr content for the formation of α′ precipitates as about 10 wt.% in low carbon steels under irradiation. Moreover, Gelles [3] reported that α′ precipitates form at much lower Cr content in Fe–Cr binary alloys following neutron irradiation. Recently, Mathon et al. [7] more precisely investigated low carbon (0.087–2.1 wt.% C) ferritic/martensitic steels with 7–12 wt% Cr following neutron irradiation using small angle neutron scattering (SANS) and showed that α′ precipitates form at more than 8 wt.% Cr. Although the formation of α′ precipitates is a major microstructural feature in high Cr ferritic/martensitic steels during neutron irradiation, their effect on the mechanical properties of these steels have not yet been systematically investigated.

In this study, the effect of Cr solute atoms and bcc Cr (α′) precipitates on edge dislocation glide in bcc Fe has been investigated using molecular dynamics (MD) simulations as a basic step toward understanding the effect of α′ formation on the mechanical properties of high Cr ferritic/martensitic steels.

## 2. Modeling method

The MD simulations use a modified version of the MDCASK code [8] with many-body interatomic potentials by Ackland et al. [9] and Finnis and Sinclair [10] to describe the atomic interactions of Fe–Fe and Cr–Cr, respectively. For the Fe–Cr interaction, the cross-potential (FeCr II) fit by Shim et al., [11] was employed. The simulation cell consists of the bcc Fe lattice, bounded by $(1\bar{1}0)$, $(1\,1\,1)$ and $(1\,1\,\bar{2})$ faces in *X*, *Y* and *Z* directions, respectively. The cell dimensions are approximately $14 \times 25 \times 28$ nm (*X*, *Y* and *Z* directions) and contain about 820 000 atoms. Periodic boundary conditions are applied in the *Y* and *Z* directions. The *X* surface is initially free, but is subject to a constant surface traction following equilibration, which provides an applied shear stress to drive dislocation motion.

An edge dislocation with $\boldsymbol{b} = a/2[1\,1\,1]$ was introduced 5 nm below the center of the cell in the *Y* direction by removing three $(3\,3\,3)$ half planes. Coherent bcc Cr precipitates were placed around the center of the cell, assuming the Cr content was 10% in the Fe lattice. The Fe content in the precipitates was set to zero, since it is not well established experimentally.

* Corresponding author. Tel.: +82 2 958 6760; fax: +82 2 958 5379.
*E-mail address:* jhshim@kist.re.kr (J.-H. Shim).

0022-3115/$ - see front matter © 2008 Elsevier B.V. All rights reserved.
doi:10.1016/j.jnucmat.2008.12.058

Before applying a shear stress to move an edge dislocation toward precipitates, the cell is equilibrated for 50 ps at 10 K. A shear stress is increased stepwise with an interval of 20 MPa after maintaining each stress for 30 ps until a dislocation detaches from a precipitate.

## 3. Results and discussion

In this study, the velocity of an edge dislocation has been measured adding Cr solute atoms to the glide planes around the dislocation core. It is found that only Cr solute atoms within 10 planes around the dislocation core effect dislocation glide. For this simulation cell and a Cr alloy content of 10%, the number of Cr atoms within the 10 planes near the dislocation glide plane is approximately 10 000. The edge dislocation starts to move at 25 MPa in the solid solution Fe–10%Cr alloy, while it starts to move at 15 MPa in pure bcc Fe.

**Table 1**
Relation between the number, size and interparticle spacing of precipitates consisting of about 10 000 Cr atoms.

| Number of precipitates | Precipitate size in diameter (nm) | Interparticle spacing (nm) |
|---|---|---|
| 1 | 6.0 | 28.1 |
| 2 | 4.9 | 14.1 |
| 3 | 4.2 | 9.4 |
| 4 | 3.8 | 7.0 |
| 5 | 3.5 | 5.6 |
| 6 | 3.3 | 4.7 |

It is assumed that all of these 10 000 Cr atoms take part in the formation of precipitates in bcc Fe and that the pure Cr precipitates have a spherical shape of given size in a row in the *Z* direction (perpendicular to the moving direction of an edge dislocation) and equal interparticle spacing. Table 1 presents the relation between the number, size and interparticle spacing of the precipitates. As the number of precipitates within the simulation cell increases from 1 to 6, the precipitate diameter decreases from 6.0 to 3.3 nm and the interparticle spacing in the *Z* direction decreases from 28.1 to 4.7 nm. First, the interaction between an edge dislocation and multiple precipitates within the simulation cell in a row in the *Z* direction (small interparticle spacing) has been investigated. It is anticipated that this precipitate configuration will have the largest critical resolved shear stress (CRSS) for edge dislocation glide due to the smaller interparticle spacings. MD snapshots in time describing the interaction between an edge dislocation and four Cr precipitates of 3.8 nm diameter are shown in Fig. 1. The edge dislocation starts to contact the precipitates 7 ps after applying a shear stress. It moves to the middle of the precipitates by cutting through the precipitates by 10 ps. Fig. 1(c) shows that the dislocation is pinned at the precipitates and bows slightly right before detachment. This demonstrates that the Cr precipitates are an obstacle to dislocation movement. The detachment process by a cutting (shear) mechanism is completely by 14 ps. The CRSS for

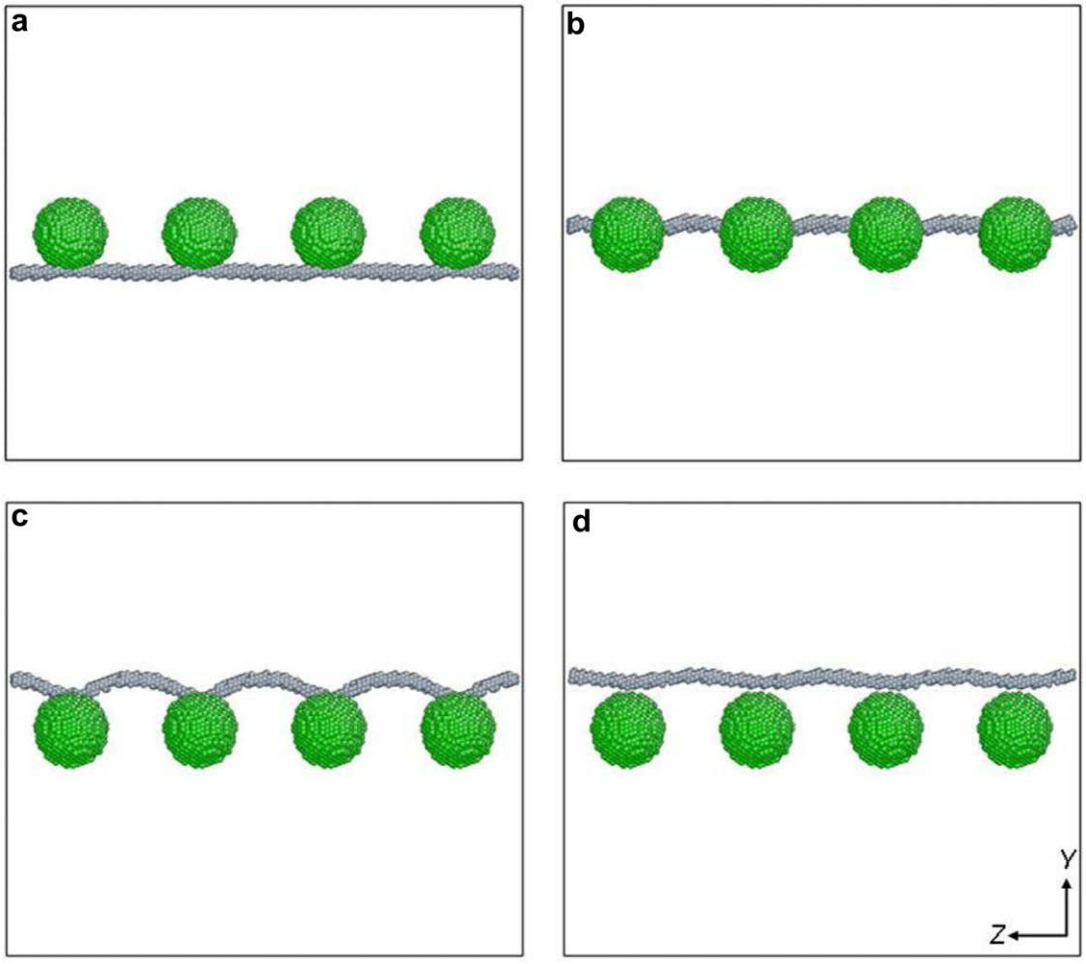


**Fig. 1.** MD snapshots of the interaction between an edge dislocation and four Cr precipitate of 3.8 nm diameter and interparticle spacing of about 7 nm at (a) 7, (b) 10, (c) 12 and (d) 14 ps.

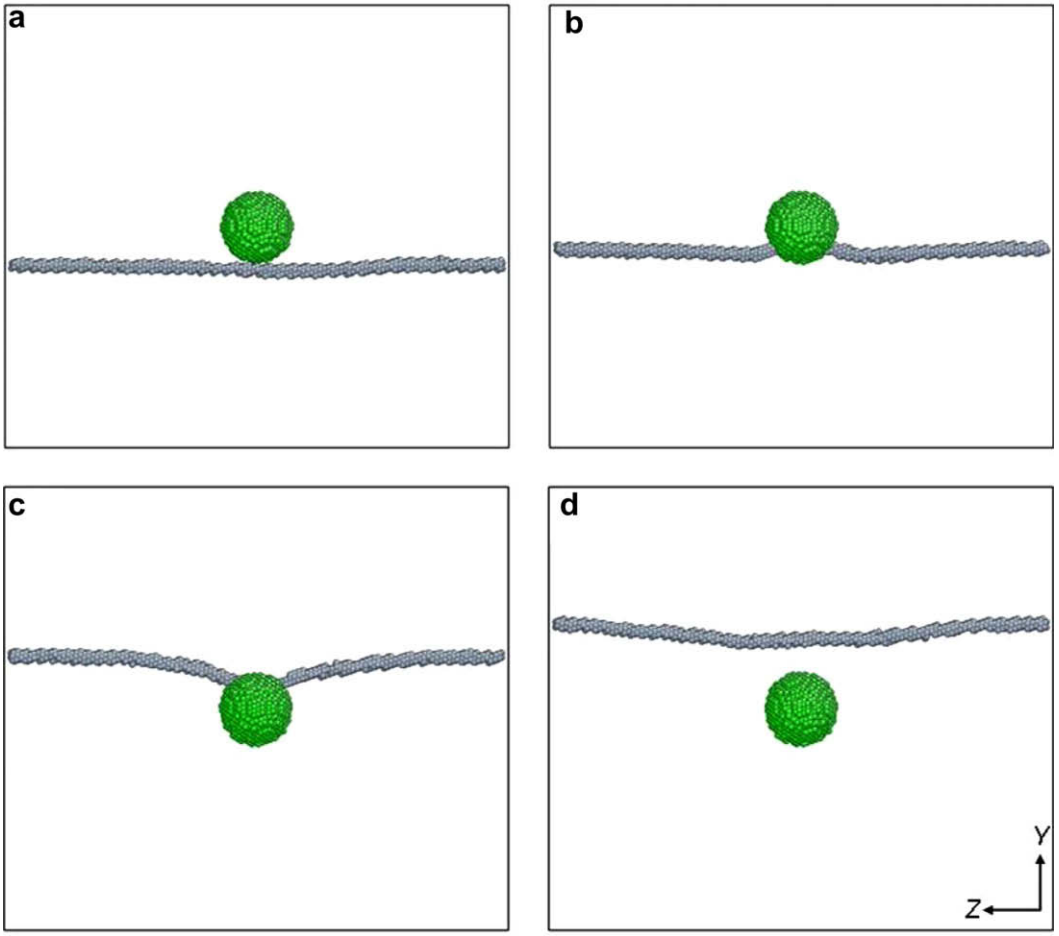


**Fig. 2.** MD snapshots of the interaction between an edge dislocation and a Cr precipitate of 3.8 nm diameter and interparticle spacing of about 28 nm at (a) 11, (b) 12, (c) 21 and (d) 24 ps.

the edge dislocation to overcome this array of regularly spaced precipitates is 240 MPa, significantly larger than for the solute strengthened Fe lattice containing 10% Cr solute atoms (25 MPa). The edge dislocation also bypasses other Cr precipitates with different precipitate size and interparticle spacing by a similar cutting mechanism.

In the case that an edge dislocation interacts with only a single precipitate in the simulation cell with an interparticle spacing of 28.1 nm, the CRSS is anticipated to be a minimum. MD simulations of precipitates of diameter from 3.3 to 6 nm have been performed with a constant precipitate interparticle spacing. MD snapshots in time describing the interaction between an edge dislocation and one Cr precipitate of 3.8 nm diameter are shown in Fig. 2. It is seen that the dislocation segment near the precipitate is absorbed into the precipitate as soon as the edge dislocation contacts the precipitate as shown in Fig. 2(b). This demonstrates an attractive force between an edge dislocation and a Cr precipitate. As the dislocation moves forward by cutting through the precipitate, it is slightly pinned around the precipitate center (Fig. 2(c)). By about 23 ps, the dislocation detaches from the precipitate at a CRSS of 60 MPa. The edge dislocation bypasses a precipitate with different size and constant interparticle spacing with the cutting mechanism and similar CRSS.

Fig. 3 plots the variation of CRSS with precipitate size. For the interaction with a single precipitate of interparticle spacing = 28.1 nm, the CRSS varies little with precipitate size. The CRSS remains constant at 60 MPa up to 4.9 nm diameter and then it slightly increases to 80 MPa for a precipitate of 6.0 nm diameter. On the other hand, the CRSS for the interaction with the precipitates at smaller interparticle spacing is very sensitive on the inter-

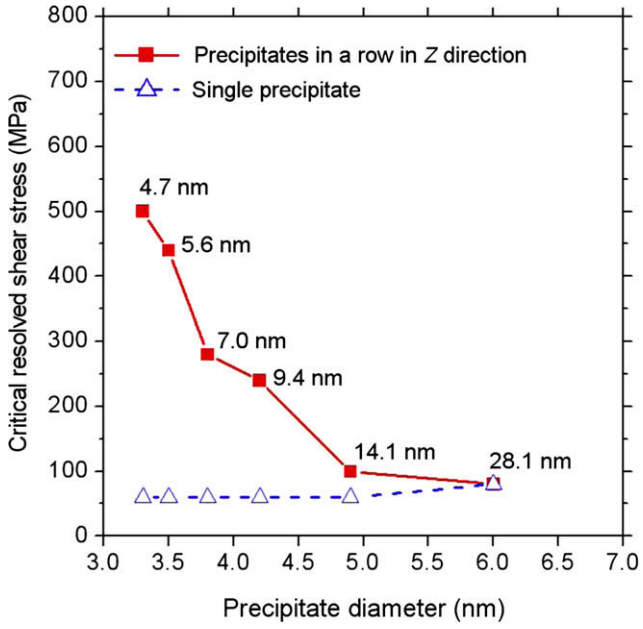


**Fig. 3.** The variation of edge dislocation CRSS as a function of Cr precipitate size. The numbers near the closed squares indicate the interparticle spacing.

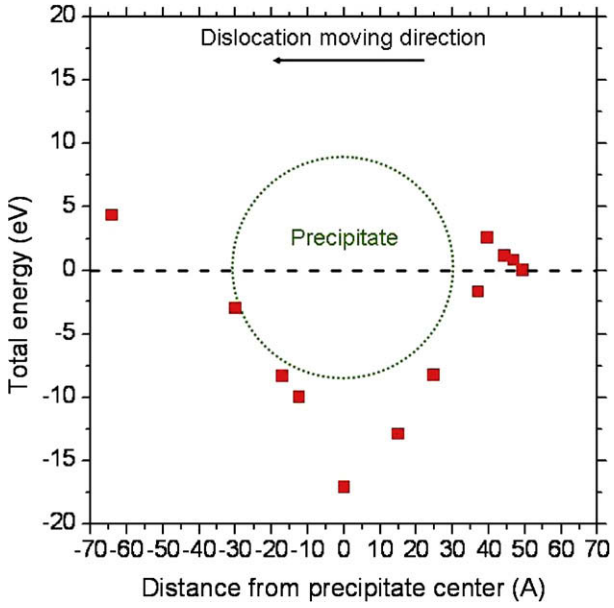


**Fig. 4.** Total system defect energy as a function of the distance of an edge dislocation from the precipitate center.

particle spacing and to a lesser extent, the precipitate size. The CRSS rapidly increases with decreasing interparticle spacing as the precipitates also become smaller. The resulting CRSS behavior is reasonably well fit by an inverse dependence on interparticle spacing, consistent with dispersed barrier hardening such as the Orowan mechanism. The CRSS reaches 500 MPa for 6 precipitates of 3.3 nm diameter separated by about 4.7 nm. These results indicate that the interparticle spacing plays a more crucial role in determining the CRSS of Fe containing Cr precipitates than the precipitate size. Assuming a random distribution of Cr precipitates at similar volume fractions and size, the CRSS should lie between the upper and lower bounds in Fig. 3.

Molecular statics (MS) calculations have been performed for a Cr precipitate and an edge dislocation, with the dislocation placed at various distances from the precipitate, to obtain the total energy versus separation distance. Fig. 4 presents the total defect energy obtained by moving the edge dislocation from the right to left in a system with a 6 nm diameter precipitate and 7 nm interparticle spacing. As seen, there is an initial repulsive interaction (increase in energy) as the dislocation approaches the precipitate, followed by a much stronger attractive interaction as the dislocation enters the precipitate. The minimum defect energy occurs when the edge dislocation is located at the precipitate center. The energy then increases as the dislocation is moved past the precipitate, resulting in a sheared precipitate and a higher defect energy associated with the newly created Fe–Cr interface. It is clear that the decrease in total energy when the dislocation is within the precipitate indicates an attractive interaction between an edge dislocation and the Cr precipitates in the MD simulations, which can provide significant strengthening depending on the precipitate size and interparticle spacing. However, the decrease in total energy is not clearly understood based only on the elastic energy of an edge dislocation, since the shear modulus of Cr is much larger than that of Fe (note that the shear moduli of Fe and Cr in the $\langle 1\,1\,1\rangle$ direction on the $\{1\,1\,0\}$ plane are 61 and 125 GPa, respectively, according to $G_{\langle 1\,1\,1\rangle\{1\,1\,0\}} = \frac{3C_{44}(C_{11}-C_{12})}{C_{11}-C_{12}+4C_{44}}$ [12]). Therefore, the decrease in total energy may be associated with dislocation core energy, interfacial energy and/or stress distribution around the precipitate, and future efforts will be directed at understanding the nature of this attractive interaction.

## 4. Conclusions

MD simulations of the interaction between an edge dislocation and nanometer-sized Cr precipitates in bcc Fe have been performed in order to understand the hardening effect of $\alpha'$ phases in high Cr ferritic/martensitic steels. The CRSS for an edge dislocation to overcome Cr precipitates has been evaluated as a function of interparticle spacing, in the limit of a single versus multiple precipitates within the simulation cell. The CRSS increases rapidly as the precipitate interparticle spacing decreases, and is consistent with dispersed barrier hardening theory that predicts an inverse dependence on interparticle spacing. The CRSS obtained for dislocation – Cr precipitate interaction are much larger than obtained for a solid solution Fe–10% Cr alloy, indicating that the precipitation of $\alpha'$ phases will strengthen high Cr ferritic/martensitic steels. MS calculations indicate an attractive interaction between the edge dislocation and Cr precipitate, that is a maximum when the edge dislocation is at the precipitate center, and that may determines the obstacle strength.

## Acknowledgements

This study has been supported by the Fundamental R&D Program for Core Technology of Materials funded by the Ministry of Knowledge Economy, Korea (2M22580), Korea Institute of Science and Technology (2E20740) and at UCB by the Office of Fusion Energy Sciences, U.S. Department of Energy, under Grant DE-FG02-04ER54750.

## References

[1] R.L. Klueh, D.R. Harries, High-Chromium Ferritic and Martensitic Steels for Nuclear Applications, American Society for Testing and Materials, West Conshohocken, PA, 2001.
[2] E.A. Little, D.A. Stow, J. Nucl. Mater. 87 (1979) 25.
[3] D.S. Gelles, J. Nucl. Mater. 108&109 (1982) 515.
[4] H. Kuwano, Y. Hamaguchi, J. Nucl. Mater. 155–157 (1988) 1071.
[5] T. Ezawa, T. Akashi, R. Oshima, J. Nucl. Mater. 212–215 (1994) 252.
[6] J.J. Kai, R.L. Klueh, J. Nucl. Mater. 230 (1996) 116.
[7] M.H. Mathon, Y. de Carlan, G. Geoffroy, X. Averty, A. Alamo, C.H. de Novion, J. Nucl. Mater. 312 (2003) 236.
[8] T. Diaz de la Rubia, M.W. Guinan, J. Nucl. Mater. 174 (1990) 151.
[9] G.J. Ackland, D.J. Bacon, A.F. Calder, T. Harry, Philos. Mag. A 75 (1997) 713.
[10] M.W. Finnis, J.E. Sinclair, Philos. Mag. A 50 (1984) 45.
[11] J.-H. Shim, H.-J. Lee, B.D. Wirth, J. Nucl. Mater. 351 (2006) 56.
[12] C.N. Reid, Deformation Geometry for Materials Scientists, Pergamon, Oxford, 1973. p. 80.